Field effect in the quantum Hall regime of a high mobility graphene wire

C. Barraud, T. Choi, P. Butti, I. Shorubalko, T. Taniguchi, K. Watanabe, T. Ihn, and K. Ensslin

Articles you may be interested in

Scaling in the quantum Hall regime of graphene Corbino devices
Appl. Phys. Lett. **104**, 203109 (2014); 10.1063/1.4878396

Integer quantum Hall effect in single-layer graphene with tilted magnetic field
J. Appl. Phys. **114**, 073705 (2013); 10.1063/1.4818605

Observation of the quantum Hall effect in epitaxial graphene on SiC(0001) with oxygen adsorption
Appl. Phys. Lett. **100**, 253109 (2012); 10.1063/1.4729824

Quantum Hall-like effect in gated four-terminal graphene devices without magnetic field
Appl. Phys. Lett. **99**, 222101 (2011); 10.1063/1.3663625

Half integer quantum Hall effect in high mobility single layer epitaxial graphene
Appl. Phys. Lett. **95**, 223108 (2009); 10.1063/1.3266524

Field effect in the quantum Hall regime of a high mobility graphene wire

C. Barraud,[1,a)] T. Choi,[1] P. Butti,[2] I. Shorubalko,[2] T. Taniguchi,[3] K. Watanabe,[3] T. Ihn,[1] and K. Ensslin[1]

[1]*Solid State Physics Laboratory, ETH Zürich, CH-8093 Zürich, Switzerland*
[2]*Swiss Federal Laboratories of Materials Science & Technologies, EMPA Elect. Metrol. Reliabil. Lab., CH-8600 Dübendorf, Switzerland*
[3]*National Institute for Materials Science, 1-1 Namiki, Tsukuba 305-0044, Japan*

In graphene-based electronic devices like in transistors, the field effect applied thanks to a gate electrode allows tuning the charge density in the graphene layer and passing continuously from the electron to the hole doped regime across the Dirac point. Homogeneous doping is crucial to understand electrical measurements and for the operation of future graphene-based electronic devices. However, recently theoretical and experimental studies highlighted the role of the electrostatic edge due to fringing electrostatic field lines at the graphene edges [P. Silvestrov and K. Efetov, Phys. Rev. B **77**, 155436 (2008); F. T. Vasko and I. V. Zozoulenko, Appl. Phys. Lett. **97**, 092115 (2010)]. This effect originates from the particular geometric design of the samples. A direct consequence is a charge accumulation at the graphene edges giving a value for the density, which deviates from the simple picture of a plate capacitor and also varies along the width of the graphene sample. Entering the quantum Hall regime would, in principle, allow probing this accumulation thanks to the extreme sensitivity of this quantum effect to charge density and the charge distribution. Moreover, the presence of an additional and counter-propagating edge channel has been predicted [P. Silvestrov and K. Efetov, Phys. Rev. B **77**, 155436 (2008)] giving a fundamental aspect to this technological issue. In this article, we investigate this effect by tuning a high mobility graphene wire into the quantum Hall regime in which charge carriers probe the electrostatic potential at high magnetic field close to the edges. We observe a slight deviation to the linear shift of the quantum Hall plateaus with magnetic field and we study its evolution for different filling factors, which correspond to different probed regions in real space. We discuss the possible origins of this effect including an increase of the charge density towards the edges. © *2014 AIP Publishing LLC*. [http://dx.doi.org/10.1063/1.4893468]

I. INTRODUCTION

Graphene is a purely 2D material with a thickness of only one carbon atom.[1] Its particular linear band structure[2] gives rise to charge carriers with unusual properties. Mobilities reaching extreme values close to $10^6 \, cm^2/Vs$ (Ref. 3) and a hybrid character between holes and electrons named charge conjugation[4] have been reported. In the quantum Hall regime,[5] the appearance of a Berry phase accumulated by the carriers during their orbital motion gives rise to a shifted sequence of the quantum Hall plateaus compared to conventional 2D systems[6,7] with a fourfold degeneracy. Most of the transport experiments in graphene-based devices have been conducted with a field-effect transistor geometry. The graphene flake is supported on a large substrate acting as a back-gate (for instance, Si/SiO_2, Si/SiO_2/hexagonal boron nitride[8] (hBN) or Si/air in the case of suspended devices). When a voltage is applied to this gate electrode, electrostatic fields exist between the graphene and the gate electrode. In the ideal case of a plate capacitor model, this electric field between the graphene and the gate electrode is homogeneous electric field and, thus, a homogeneous charge

density is induced. However, because of the finite lateral size[9] of the graphene flake and because of its finite density of states at all energy, edge effects are present leading to charge accumulation at the graphene edges (see Fig. 1(a)). The value of the capacitance can, thus, strongly deviates[10,11] from the plate capacitor model (Fig. 1(b)). This effect has been recently evoked[12–14] in experimental studies involving high quality graphene devices (suspended and supported on hBN) in the quantum Hall regime in which only edge states propagate. In this study, we will use a similar approach (i.e., high quality graphene wire in the quantum Hall regime). We will also distinguish between the different filling factors, which may give spatial resolution for the measured capacitance at high magnetic field.

II. DEVICE FABRICATION AND TRANSPORT MEASUREMENTS UNDER MAGNETIC FIELD

Using e-beam lithography, our device is contacted by two Ohmic contacts (Cr 0.5 nm/Au 45 nm) deposited on a bilayer graphene flake, which is itself deposited on a local hBN flake sitting on a large Si/SiO_2 substrate (the thickness of the oxide is 285 nm). The graphene flake is obtained by exfoliation from graphite on a PMMA (200 nm)/PVA (100 nm) double-layer and identified by optical microscopy.

a)Author to whom correspondence should be addressed. Electronic addresses: cbarraud@phys.ethz.ch or clement.barraud@univ-paris-diderot.fr.

(a)

(b)
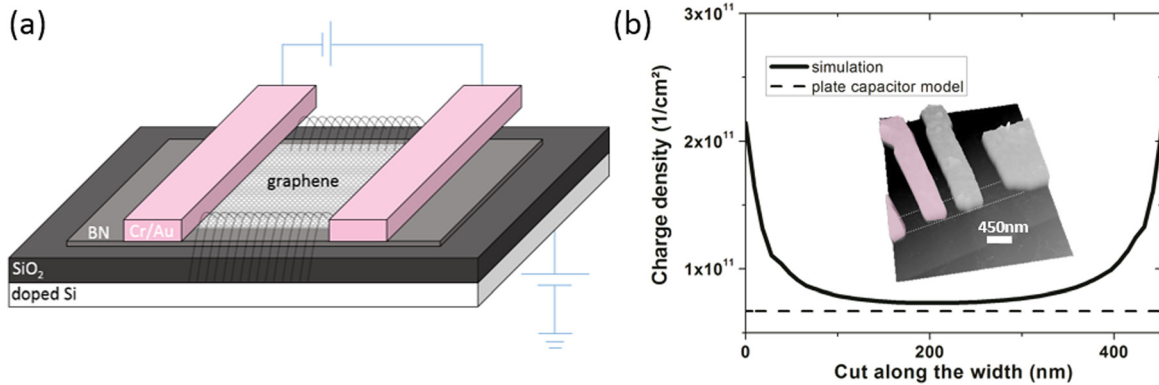
FIG. 1. (a) Graphene wire supported on boron nitride substrate. The thickness of the SiO_2 layer is 285 nm and 31 nm for the hBN local substrate. Field lines coming from the Si/SiO_2 back-gate participating to the electrostatic edge focusing effect are represented in black dotted lines. (b) Simulated charge density profile along the width of the graphene flake (1 V applied to the back-gate electrode). Solid black line represents the simulation including effects of the fringing field lines. Dashed line represents the value for the plate capacitor model. (Inset) Scanning force microscope image of the measured device. The graphene wire's edges are outlined with the white dashed line.

It is then characterized by atomic force microscopy (AFM) and subsequently transferred onto a hBN flake of 34 nm thickness using the transfer technique.[15] For this study, we selected a graphene wire, naturally defined, 460 nm in width and several tens of micrometers in length. The hBN surface is characterized by AFM prior to the transfer to ensure a high quality topography (very low roughness, no structural defects, no contamination). The roughness is found to be <0.1 nm (limited by the resolution of our AFM) over a large area ($>20 \times 20 \, \mu m^2$). This is one requirement[15] to observe a high mobility of charge carriers in graphene. The separation between the Ohmic contacts is also reduced to match the width of the graphene flake (i.e., 460 nm). Under these conditions, well-defined quantum Hall plateaus can be observed[16] in a two-terminal configuration, which is another requirement for this study. At the end of the fabrication process, the device is annealed under a controlled atmosphere of Ar/H_2 (ratio of the gas flows: 10/1) at temperatures up to 300 °C during 5 h. This step was found[15,17] to be crucial to remove lithographic residues such as the PMMA used, for instance, for e-beam lithography and from the transfer film and thus to decrease residual doping in the system and to improve its transport properties. An AFM image of the final device after annealing is shown in the inset of Fig. 1(b). The two contacts used in this study, which fulfill the geometric condition, are represented in pink. The two other contacts are floating during the transport experiment.

The device is measured in a variable temperature insert designed for low-noise transport experiments. All measurements shown here were obtained at a temperature of 2.5 K in a two-terminal configuration. Superimposed DC ($V = 250 \, \mu V = linear \, regime$) and AC ($dV = 200 \, \mu V$) voltages were applied to the sample. AC signals are used to extract the differential conductance G given by dI/dV (dI was measured by sending the response signal through an I-V converter). Fig. 2(a) shows a map, where dG/dV_{bg} is plotted as a function of back-gate voltage (= density) and magnetic field applied perpendicularly to the graphene plane. Black regions correspond to plateaus of conductance formed in the quantum Hall regime. The observed sequence corresponds to

the series expected for bilayer graphene (± 4, ± 8, ± 12, ± 16, $\pm 20 \, e^2/h$...). Some plateaus corresponding to broken symmetry (spins and valleys) states[18] also appear like those at 0, -1, ± 2, and $-3 \, e^2/h$. The mobility of charge carriers has been estimated to be around 35 000 cm^2/V.s in our system from the appearance of Shubnikov-de Haas oscillations around 250 mT.[19] The residual doping has been observed to be low as the Landau fan is well centered at 0 V in back-gate voltage.

In this device geometry and assuming a plate capacitor model, quantum Hall plateaus of a particular filling factor are expected to shift linearly with magnetic field and gate voltage (= charge density). However, we observe, in Fig. 2(a), a slight deviation especially visible for the plateaus at 3 and 4 e^2/h in the hole transport regime for which the plateau positions seem to bend (evolution for different filling factors assuming a plate capacitor is also plotted as a guide for the eyes). Such a deviation has been recently interpreted[20] as the effect of charge accumulation at the graphene edges. In the following, we will comment on this observation and discuss its possible origins.

III. ANALYSIS OF THE QUANTUM HALL PLATEAUS SHIFT

We start by applying the method originally developed by Vera-Marun *et al.*[12] after similar observations reported in both supported and suspended graphene devices. In the quantum Hall regime and when the Fermi energy lies in-between two Landau levels, conduction is governed by propagating edge states of well-defined conductance, whereas the "bulk" part of the graphene flake is insulating.[5] An estimate[12] of the lateral region probed by the charge carriers in those edge channels is given by the cyclotron diameter of the highest occupied Landau level $d = \sqrt{\frac{\nu h}{e \pi B}}$, where ν is the filling factor and B is the magnetic field. As mentioned before, electrostatic fringe fields are expected to result in charge accumulation at the edges of the device. This leads to an inhomogeneous charge density profile along the width of the
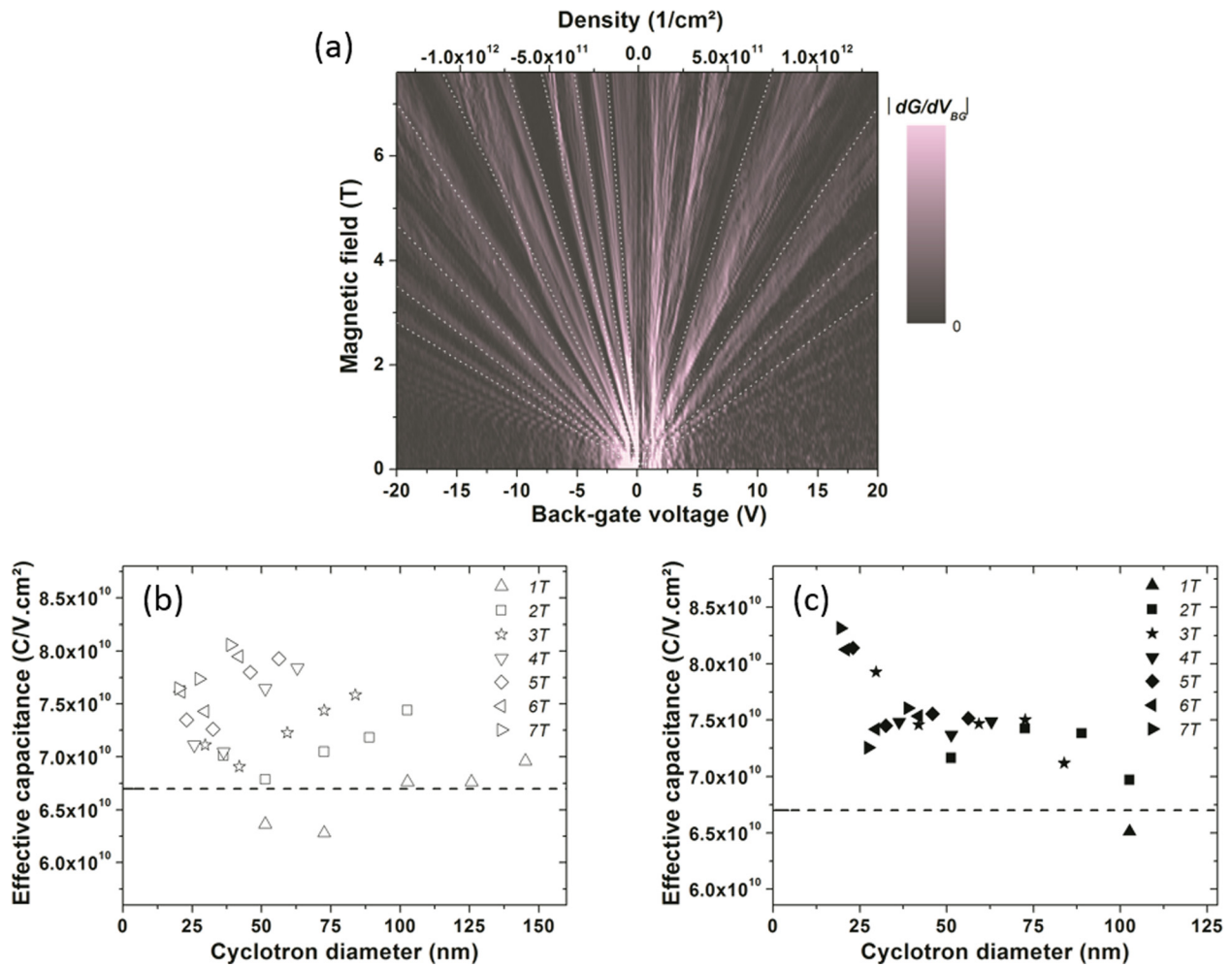
FIG. 2. (a) Conductance mapping in the quantum Hall regime of the bilayer graphene wire. A regular sequence is observed for bilayer graphene (4, 8, 12, 16e²/h…). Additional plateaus corresponding to broken symmetries states at 0, −1, ±2, and −3 e²/h also appear. White dotted lines represent the expected evolution for the different plateaus (center) for filling factor −20, −16, −12, −8, −6, −4, −3, −2, −1, 4, 8, 12, and 16. (b) and (c) Shift of the effective capacitance per area as a function of the cyclotron diameter for the hole and electron side, respectively, and for different values of the magnetic field. The solid line corresponds to the value of the capacitance obtained with a standard plate capacitor model.

flake as shown before in Fig. 1(b). Electrostatic equations describing this dependence can be found in Refs. 10 and 11 (graphene is taken as an ideal metal, the effect of magnetic field and of finite density of states on the screening properties of the graphene are also neglected). This effect is significant and differences between the charge density in the middle of the flake and at the edges could, in principle, reach several hundreds of percents.[10–12] Within this study, finite elements simulations predicted a notable change of the local effective capacitance per area (= C_v^*) from 1.12×10^{-8} C/V.cm² in the center of the flake to 3.30×10^{-8} C/V.cm² at the edges.

As in the quantum Hall regime, the charge density and magnetic field are linked for the different filling factors by the following equation:

$$n_\nu = \nu \frac{eB}{h} ,$$ (1)

we can follow the evolution of the effective local capacitance (= C_v^*) ($n_\nu = C_\nu^* (V_{bg} - V_{Dirac})/e$) with respect to the applied magnetic field as plotted in Fig. 2(a).

Following the procedure described in Ref. 12, we plot in Figs. 2(b) and 2(c) the evolution of the effective capacitance par area C^* (the center of each plateau V_{bg} is extracted from the data at different magnetic fields. Corresponding n_ν are then calculated following equation (1) and C^* is finally also calculated) as a function of the cyclotron diameter for different magnetic fields ranging from 1 to 7 T. In their approximation, the cyclotron diameter was expected to give a rough estimation of the distance of the edge state from the edge of the sample. The two Figs. 2(b) and 2(c) correspond to the holes transport regime and electrons transport regime, respectively. We can observe the tendency of a gradual increase of the effective capacitance as the charge carriers are pushed towards the edges (i.e., decreasing cyclotron diameter = increasing magnetic field). This variation is however, in the present study, moderate (≤20%) compared to the simulations (>100%). In a less extent, this was also observed in Ref. 12, where scaling factors of 0.8 (for a suspended bilayer flake of 0.4 μm width and 2.6 μm length) and 0.7 (for a monolayer graphene flake of 2 μm width and 2.5 μm length supported on hBN) were used to fit the experimental data. Here, one has to remember that the modeling assumes that

the top electrode is an ideal metal, which is certainly not the case with graphene under high magnetic field. As mentioned before, the graphene plane is composed of insulating and conducting parts. It is, thus, expected not to fit correctly the experimental data with the simulated capacitance profile, which assumes a fully metallic plane.

IV. DISCUSSION

We now try to understand the possible origin of this phenomenon by starting from the model of charge accumulation at the edges. In the picture of compressible and incompressible stripes,[21] edge channels act like parallel charge waveguides. This model is only valid in the case of a smooth edge confinement potential, in which the edge channels can reconstruct. This may not be the case realized in graphene, where edges are naturally atomically sharp, and the density profile may change rather abruptly at the sample edge because there is no band gap in the material. Assuming that the increase of capacitance is due to the charge accumulation, edge states of different filling factors should however probe different regions[22] of the graphene flake and, thus, in principle, should "feel" different effective density regions and also different variations with magnetic field. The lowest filling factor is the closest to the edge and should, thus, see the highest effective capacitance variation as a function of magnetic field). In Figs. 3(a) and 3(b), the data presented previously in Figs. 2(b) and 2(c) are plotted now as a function of magnetic field and for different filling factors (positive and negative), which are specified in the figures.

We first observe that the previous expectation (highest capacitance variation for the lowest filling factors) is not fulfilled. At a given magnetic field, an apparent random order is observed. The lowest filling factor is here not even associated to the highest value of the effective capacitance. For negative filling factors, the situation seems to be even the opposite. At this point, one may argue that the positions in real-space of the different wave-functions are not easy to determine as described in Ref. 22 and could even overlap between the forward and backward channels for very narrow ribbons. In Figs. 3(c) and 3(d), we show the cyclotron diameter dependence for the different filling factors. We notice that all the effective capacitance associated with different filling factors increase with their cyclotron diameter. They all start from the same value close to the one obtained with a plate capacitor model $(1.07 \times 10^{-8}\,\mathrm{C/V.cm^2})$ and then, surprisingly, they all reach roughly the same maximum value. Interestingly, we also observe a continuous increase of the capacitance for the negative filling factors whereas, for positive filling factors (+4, +8, +12, and +16), the plot shows a linear increase up to 3 T and, then, a saturation. From the electrostatic point of view, one would expect e-h symmetry
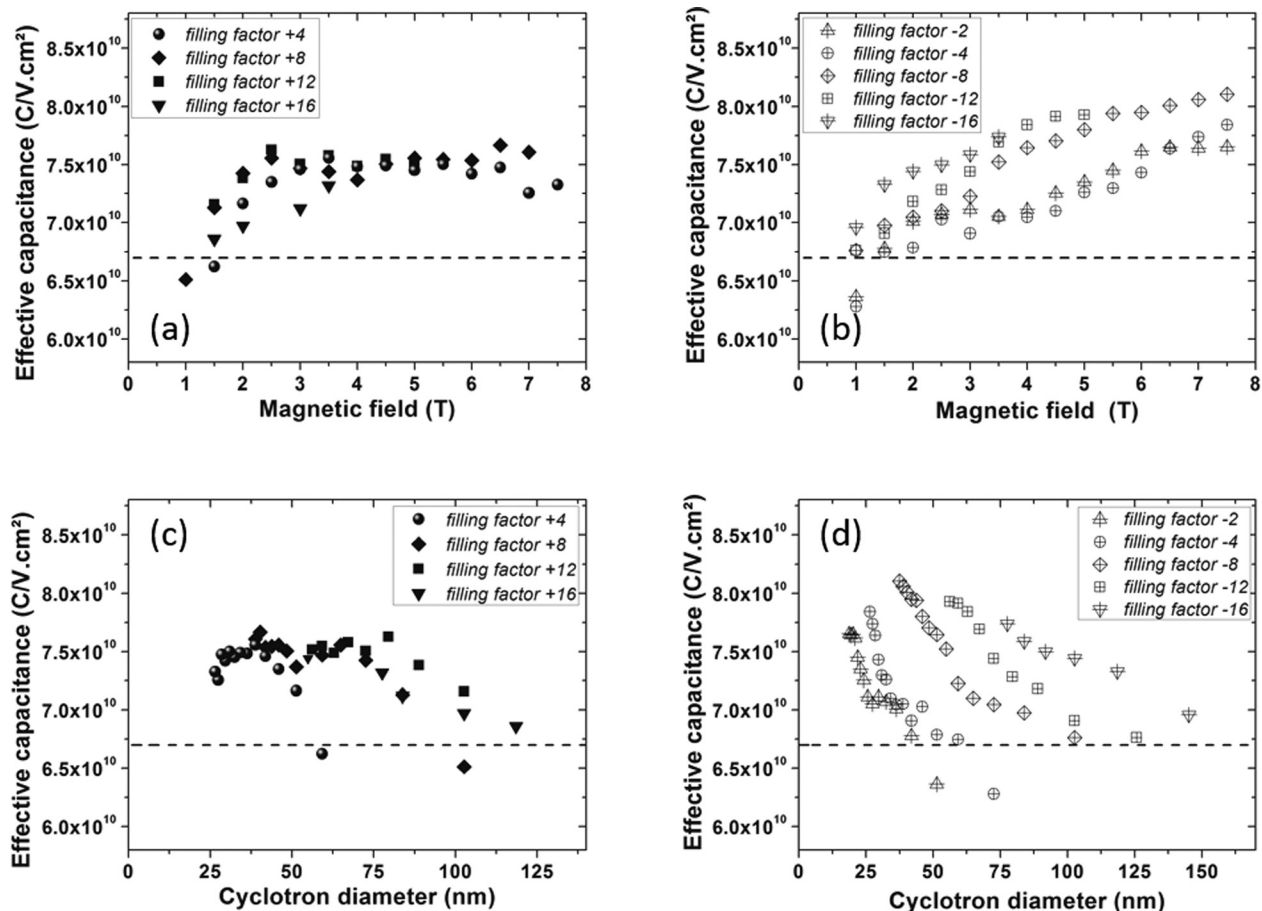
FIG. 3. (a) and (b) Effective capacitance per area versus magnetic field obtained for the different filling factors (electrons = filled symbols and holes = empty symbols, respectively). (c) and (d) Effective capacitance per area versus cyclotron diameter plotted for the different filling factors. The dashed line represents the value of the capacitance obtained in the framework of a plate capacitor model.

but effects of localized trapped charges in the SiO_2 substrate could be relevant.[23,24]

The charge accumulation is expected to be a universal behavior. However, here we observe that the effect of charge accumulation is quite reduced in agreement with the observation of Vera-Marun *et al.*[12] and that the different filling factors feel roughly the same capacitance profile (which cannot be compared with Ref. 12 as there was no discrimination between the different filling factors). Alternative and/or competing phenomena could thus be invoked to explain this observation. For instance, the quantum capacitance[25,26] (which is not taken into account in the simulation) could also lead to a non-linear dependence of the density on gate voltage. Another alternative could be related to the formation of localized states[27] at higher magnetic fields. If the width of the quantum Hall plateaus, which depends on the presence of localized states in the bulk of the sample, changes non-linearly with gate voltage ($=$ density); then, one would also observe such non-linearities. Also, the effect of band structure at the graphene edges is unknown. Theoretically, it can be assumed that the density can increase up to the last row of carbon atoms but the electronic structures and, thus, the density of states also strongly depends on the edge configuration,[28] which may certainly vary here at the scale of the device. An experimental effort has to be made in this direction to control it. Finally, the effect of spin-orbit coupling in bilayer graphene has been predicted to bend also the different Landau levels.[29]

V. CONCLUSION

In this paper, we have investigated the effect of electrostatic fringe fields at the sample edge by employing quantum Hall edge channels. We have followed the behavior of different states corresponding to different regions probed in the real space. A complex behavior is then observed, which could highlight the fact that charge density profile is not entirely dominated by the charge accumulation effect. Further investigations should be performed by checking the role of the thickness of the dielectric used for gating and different device geometries.

ACKNOWLEDGMENTS

[1]A. Geim and K. Novoselov, Nature Mater. **6**, 183 (2007).
[2]A. H. Castro Neto, N. M. R. Peres, K. S. Novoselov, and A. K. Geim, Rev. Mod. Phys. **81**, 109 (2009).
[3]X. Du, I. Skachko, A. Barker, and E. Y. Andrei, Nat. Nanotechnol. **3**, 491 (2008).
[4]M. I. Katsnelson and K. S. Novoselov, Solid State Commun. **143**, 3 (2007).
[5]K. Von Klitzing, Rev. Mod. Phys. **58**, 519 (1986).
[6]K. S. Novoselov, E. McCann, S. V. Morozov, V. I. Fal'ko, M. I. Katsnelson, U. Zeitler, D. Jiang, F. Schedin, and A. K. Geim, Nat. Phys. **2**, 177 (2006).
[7]Y. Zhang, Y.-W. Tan, H. L. Stormer, and P. Kim, Nature **438**, 201 (2005).
[8]T. Taniguchi and K. Watanabe, J. Cryst. Growth **303**, 525 (2007).
[9]M. C. Hegg and A. V. Mamishev, in *Proceedings of the Conference Record of the 2004 International Symposium on Electrical Insulating* (2004), pp. 384–387.
[10]P. Silvestrov and K. Efetov, Phys. Rev. B **77**, 155436 (2008).
[11]F. T. Vasko and I. V. Zozoulenko, Appl. Phys. Lett. **97**, 092115 (2010).
[12]I. J. Vera-Marun, P. J. Zomer, A. Veligura, M. H. D. Guimarães, L. Visser, N. Tombros, H. J. van Elferen, U. Zeitler, and B. J. van Wees, Appl. Phys. Lett. **102**, 013106 (2013).
[13]H. Hettmansperger, F. Duerr, J. B. Oostinga, C. Gould, B. Trauzettel, and L. W. Molenkamp, Phys. Rev. B **86**, 195417 (2012).
[14]D. Bischoff, T. Kräuhenmann, S. Dröscher, M. A. Gruner, C. Barraud, T. Ihn, and K. Ensslin, Appl. Phys. Lett. **101**, 203103 (2012).
[15]C. R. Dean, A. F. Young, I. Meric, C. Lee, L. Wang, S. Sorgenfrei, K. Watanabe, T. Taniguchi, P. Kim, K. L. Shepard, and J. Hone, Nat. Nanotechnol. **5**, 722 (2010).
[16]D. Abanin and L. Levitov, Phys. Rev. B **78**, 035416 (2008).
[17]C. R. Dean, A. F. Young, P. Cadden-Zimansky, L. Wang, H. Ren, K. Watanabe, T. Taniguchi, P. Kim, J. Hone, and K. L. Shepard, Nat. Phys. **7**, 693 (2011).
[18]B. E. Feldman, J. Martin, and A. Yacoby, Nat. Phys. **5**, 889 (2009).
[19]A. S. Mayorov, D. C. Elias, I. S. Mukhin, S. V. Morozov, L. A. Ponomarenko, K. S. Novoselov, A. K. Geim, and R. V. Gorbachev, Nano Lett. **12**, 4629 (2012).
[20]H. J. van Elferen, A. Veligura, E. V. Kurganova, U. Zeitler, J. C. Maan, N. Tombros, I. J. Vera-Marun, and B. J. van Wees, Phys. Rev. B **85**, 115408 (2012).
[21]D. B. Chklovskii, B. I. Shklovskii, and L. I. Glazman, Phys. Rev. B **46**, 4026 (1992).
[22]A. A. Shylau, I. V. Zozoulenko, H. Xu, and T. Heinzel, Phys. Rev. B **82**, 121410 (2010).
[23]H. Wang, Y. Wu, C. Cong, J. Shang, and T. Yu, ACS Nano **4**, 7221 (2010).
[24]G. Kalon, Y. J. Shin, V. G. Truong, A. Kalitsov, and H. Yang, Appl. Phys. Lett. **99**, 083109 (2011).
[25]Z. Chen and J. Appenzeller, IEEE Int. Electron Devices Meet. **2008**, 1–4.
[26]S. Dröscher, P. Roulleau, F. Molitor, P. Studerus, C. Stampfer, K. Ensslin, and T. Ihn, Phys. Scr. **T146**, 014009 (2012).
[27]J. Martin, N. Akerman, G. Ulbricht, T. Lohmann, K. von Klitzing, J. H. Smet, and A. Yacoby, Nat. Phys. **5**, 669 (2009).
[28]A. Akhmerov and C. Beenakker, Phys. Rev. B **77**, 085423 (2008).
[29]F. Mireles and J. Schliemann, New J. Phys. **14**, 093026 (2012).